A Generalized Approach for Computing Most Sensitive Eigenvalues With Respect to System Parameter Changes in Large-scale Power Systems

C. Y. Chung, *Senior Member, IEEE*, and Bo Dai, *Member, IEEE*

Abstract—**The recently-developed Two-sided Arnoldi and Sensitive Pole Algorithm (TSA-SPA) is effective and robust in computing the most sensitive eigenvalues with respect to control parameter changes in large-scale power systems. This paper extends the TSA-SPA to handle different system parameters, including control, system operating and network parameters. The proposed algorithm makes use of perturbation in reduced matrix obtained from Arnoldi/TSA method through linearization and successfully avoids the need for TSA-SPA to formulate the whole state matrix of the system and to explicitly calculate the elements' variations in system state matrix. A new deflation method is also proposed and adopted in the generalized algorithm to find other sensitive eigenvalues. Simulation results illustrate that the generalized algorithm is able to not only maintain the excellent properties of TSA-SPA in terms of convergence and robustness, but also consider various parameter changes effectively in large-scale power systems.**

***Index Terms*—Eigenvalues, sensitivity, large-scale power systems, small-signal stability problems.**

I. Introduction

EIGENVALUE methods are an effective means to analyze oscillation problems in power systems [1-10]. The traditional model-based methods, which perform the eigenvalue analysis through linearizing the dynamic model of the power system, have been widely used. With the advent of phasor measurement unit (PMU) technology, measurement-based modal analysis methods [11-12] have been proposed recently. Real-time signals measured from PMUs are analyzed to estimate dominant eigenvalues and correlations between dominant eigenvalues and changes of system operating conditions can also be established. Measurement-based methods have successfully solved the problems of model-based methods, including uncertainty of models and long computing time, but their performance and system information entirely depend on the signals captured by PMUs. Observability of PMUs on dominant eigenvalues changes with operating conditions. Development of a reliable monitoring system with a suitable number and locations of PMUs to robustly capture dominant and specified eigenvalues is a very challenging task. Besides, measurement based methods may not capture the well-damped eigenvalues which can provide useful information to the operator. Research on both model-based and measurement-based methods is necessary to achieve complementary solutions although this paper focuses on model-based methods.

Based on the linearized power system model, complete eigenvalues computation can be realized by the well-known QR method, which has high numerical stability and accuracy. When applied to large systems, it becomes inefficient owing to it being incapable of incorporating sparsity techniques [13]. Moreover, in most applications, there is no need to calculate the whole set of eigenvalues like the QR method does. Therefore, selective eigenvalue computation methods have been developed to focus on calculating only some eigentriples (eigenvalues and the corresponding right and left eigenvectors) of interest. Analysis of Essentially Spontaneous Oscillations in Power Systems (AESOPS) [14] and the subsequent Program for Eigenvalue Analysis of Large Systems (PEALS) algorithm [15] are proposed to compute electro-mechanical modes of oscillation for large power systems. S-Method [16] is efficient for finding the unstable modes. Sequential Two-stage Eigen analysis for Power Systems (STEPS) [17] can be used for computing eigenvalues for a small study zone. Dominant Pole Algorithm (DPA) effectively computes the eigenvalues dominant in power system transfer functions [18].

Eigenvalue sensitivity analysis can evaluate the impact of system parameters' changes on the specified eigenvalues, which are related to oscillation problems, and provide a guideline on the magnitude and direction of the parameters' changes to solve the problems. These system parameters include control parameters of controllers; system operating parameters, such as generators' outputs and loads; and system network parameters, such as reactance of transmission lines. Eigenvalue sensitivity has been widely applied in control coordination, generation redispatch and other applications in power system analyses. In large-scale power systems,

This work was supported by the Department of Electrical and Computer Engineering of the University of Saskatchewan and the Department of Electrical Engineering of The Hong Kong Polytechnic University.

C.Y. Chung is with the Department of Electrical and Computer Engineering, University of Saskatchewan, Saskatoon, SK S7N 5A9, Canada (email: c.y.chung@usask.ca)

Bo Dai is with the Department of Electrical Engineering, The Hong Kong Polytechnic University, Hung Hom, Hong Kong (email: bo.dai@polyu.edu.hk).

eigenvalues with high sensitivity with respect to system parameters are normally focused upon because only limited eigenvalues can be calculated. Sensitive Pole Algorithm (SPA) [19] has been proved successful for finding the most sensitive eigenvalues with respect to changes of control parameters in large-scale power systems. Arnoldi method [20] is a powerful method, which has been widely used for computing eigenvalues of large matrices in specified regions, through matrix reduction, but it uses one Krylov subspace in the calculation so only right eigenvectors can be computed. Two-Sided Arnoldi method (TSA) is a two-sides subspace method [17], which can effectively obtain both right and left eigenvectors. By integrating SPA with TSA, the Two-sided Arnoldi and Sensitive Pole Algorithm (TSA-SPA) [21] is proposed to compute sensitive eigenvalues for a specified region of interest in complex plane and the corresponding eigenvectors in a more efficient way, especially in large-scale power systems.

However, both SPA and TSA-SPA are limited to changes of control parameters and they cannot be directly applied to other types of system parameters such as operating parameters and network parameters. To consider the perturbation on these system parameters, the whole state matrix needs to be formed explicitly and the sparsity of the state matrix is destroyed, making eigenvalue computation by either of the two methods infeasible for large-scale systems.

This paper extends TSA-SPA to a generalized method, which can compute most sensitive eigenvalues with respect to different types of system parameters. The generalized method first reduces the initial problem to a much smaller dimension by using TSA and then the sensitive eigenvalues are computed in SPA by iterative vectors' updating associated with the perturbation of the reduced matrix. Formulation of the whole state matrix is avoided and the generalized method is able to find the most sensitive eigenvalues to changes of different types of system parameters with excellent convergence and robustness. Finally, a new deflation method is developed to find several other sensitive eigenvalues with the generalized method.

The rest of this paper is organized as follows. Section II covers background of the proposed algorithm. Section III introduces the generalized TSA-SPA algorithm. The effectiveness of the proposed algorithm is demonstrated in a small power system in Section IV and a large-scale power system in Section V. Finally, conclusions are provided in Section VI.

II. BACKGROUND

The mathematical model of a linearized single-input single-output (SISO) dynamic system around an operating point can be expressed as [22]:

$$\begin{cases} \dot{\boldsymbol{z}}(t) = \boldsymbol{A}\boldsymbol{z}(t) + \boldsymbol{b}u_{in}(t) \\ y_{out}(t) = \boldsymbol{c}^*\boldsymbol{z}(t) + Du_{in}(t) \end{cases} \tag{1}$$

where $\boldsymbol{A} \in \mathfrak{R}^{n\times n}$ is the state matrix, $\boldsymbol{z}(t) \in \mathfrak{R}^n$ is the state vector, $u_{in}(t)$ is the input variable, $y_{out}(t)$ is the output variable, $\boldsymbol{b} \in \mathfrak{R}^n$ is the input column vector, $\boldsymbol{c} \in \mathfrak{R}^n$ is the output column vector and $D \in \mathfrak{R}$ is the direct transmission matrix of unit rank. Without loss of generality, $D = 0$. Superscript * denotes the conjugated transpose function.

A. Brief Overview of TSA-SPA

Transfer function $\boldsymbol{H}(s)$ of the dynamical system in (1) can be expressed as a sum of residues $R \in \mathbb{C}$ over finite first-order k poles. Commonly, poles with small residues are neglected due to the small influence on the transfer function [18].

$$\boldsymbol{H}(s) \cong \sum_{i=1}^{k} \frac{R_i}{s-\lambda_i} \tag{2}$$

where the residues are

$$R_i = (\boldsymbol{c}^*\boldsymbol{x}_i)(\boldsymbol{y}_i^*\boldsymbol{b}) \tag{3}$$

and vectors $\boldsymbol{x}_i$, $\boldsymbol{y}_i$ denote the corresponding right and left eigenvectors, respectively, of pole λ_i.

Besides, the eigenvalue sensitivity of a parameter p can be determined by:

$$\frac{\partial\lambda_i}{\partial p} = \boldsymbol{y}_i^* \frac{\partial \boldsymbol{A}}{\partial p}\boldsymbol{x}_i \tag{4}$$

The eigenvalue with the largest sensitivity can be calculated in SPA [19] by computing the pole with the largest residue of a modified dynamic system where $\boldsymbol{b} = (\partial\boldsymbol{A}/\partial p)\boldsymbol{x}_i$ and $\boldsymbol{c} = (\partial\boldsymbol{A}^*/\partial p)\boldsymbol{y}_i$, making the largest residue $R_i = (\boldsymbol{c}^*\boldsymbol{x}_i)(\boldsymbol{y}_i^*\boldsymbol{b}) = (\boldsymbol{y}_i^*(\partial\boldsymbol{A}/\partial p)\boldsymbol{x}_i)^2$ in accord with the eigenvalue with the largest sensitivity. The detailed proof can be referred to in [19].

In the widely-used Arnoldi method [23], Krylov subspace $\boldsymbol{V}_k$ of k dimensions is firstly built and eigenpairs are then computed from the $k\times k$ upper Hessenberg matrix $\boldsymbol{H}_k$. Since the upper Hessenberg matrix is much smaller than Matrix $\boldsymbol{A}$, the Arnoldi method is very effective in solving large-scale eigenvalue problems. In TSA method, the orthogonal projections of Matrices $\boldsymbol{A}$ and $\boldsymbol{A}^T$ are executed independently, where T denotes the transpose function in this paper. Bases for the two Krylov subspaces $\boldsymbol{V}_k = [\boldsymbol{v}_1, \boldsymbol{v}_2, \dots, \boldsymbol{v}_i, \dots, \boldsymbol{v}_k]$ and $\boldsymbol{W}_k = [\boldsymbol{w}_1, \boldsymbol{w}_2, \dots, \boldsymbol{w}_i, \dots, \boldsymbol{w}_k]$ are built independently. As long as $\boldsymbol{U}_k = \boldsymbol{W}_k^*\boldsymbol{V}_k$ has full rank, i.e. $\det(\boldsymbol{U}_k) \neq 0$, the reduced matrices $\widehat{\boldsymbol{H}}_k$ ($\widehat{\boldsymbol{H}}_k \equiv \boldsymbol{U}_k^{-1}\boldsymbol{W}_k^*\boldsymbol{A}\boldsymbol{V}_k$) and $\widehat{\boldsymbol{M}}_k$ ($\widehat{\boldsymbol{M}}_k \equiv \boldsymbol{W}_k^*\boldsymbol{A}\boldsymbol{V}_k\boldsymbol{U}_k^{-1}$) can always be obtained. It is deduced that $\widehat{\boldsymbol{H}}_k \equiv \boldsymbol{H}_k$ and $\widehat{\boldsymbol{M}}_k \equiv \boldsymbol{M}_k$ once TSA converges, where $\boldsymbol{H}_k$ and $\boldsymbol{M}_k$ satisfy (5) and (6), respectively.

$$\boldsymbol{A}\boldsymbol{V}_k = \boldsymbol{V}_k\boldsymbol{H}_k \tag{5}$$

$$\boldsymbol{A}^T\boldsymbol{W}_k = \boldsymbol{W}_k\boldsymbol{M}_k \tag{6}$$

Eigenvalues with the largest modulus and the corresponding right and left eigenvectors can therefore be calculated based on the reduced matrices $\widehat{\boldsymbol{H}}_k$ and $\widehat{\boldsymbol{M}}_k$.

With suitable preconditions, transformations such as shift-invert transformation [23] applied to Matrix $\boldsymbol{A}$, the computation of eigenvalues with the largest modulus can be converted into eigenvalues close to a specified shift point σ. By selecting the shift point, eigenvalues in different specified regions can be calculated and studied. The details of TSA can referred to in [24].

In TSA, eigenvectors corresponding to the calculated eigenvalue λ_i can be easily obtained by $\boldsymbol{x}_i = \boldsymbol{V}_k\boldsymbol{x}_{ri}$ and $\boldsymbol{y}_i =$

$\boldsymbol{W}_k\boldsymbol{y}_{ri}$, where $\boldsymbol{x}_{ri}$ and $\boldsymbol{y}_{ri}$ are eigenvectors of reduced matrices $\widehat{\boldsymbol{H}}_k$ and $\widehat{\boldsymbol{M}}_k$, respectively, with dimensions $k \times k$. Thus, the sensitivity of eigenvalues to the control parameter in (4) can be rewritten in the following form:

$$\frac{\partial \lambda_i}{\partial p} = \boldsymbol{y}_i^* \frac{\partial \boldsymbol{A}}{\partial p} \boldsymbol{x}_i = \boldsymbol{y}_{ri}^* \boldsymbol{W}_k^* \frac{\partial \boldsymbol{A}}{\partial p} \boldsymbol{V}_k \boldsymbol{x}_{ri} \tag{7}$$

It has been proved in TSA-SPA [21] that the eigenvalue with the largest sensitivity can be calculated by setting $\boldsymbol{b} = \boldsymbol{U}_k^{-1}\boldsymbol{W}_k^* \frac{\partial \boldsymbol{A}}{\partial p}\boldsymbol{V}_k$ and $\boldsymbol{c} = \boldsymbol{W}_k^* \frac{\partial \boldsymbol{A}}{\partial p}\boldsymbol{V}_k \boldsymbol{U}_k^{-1}$. The detailed proof can be referred to in [21]. The procedure of TSA-SPA is shown in Alg. 1 as follows.

Algorithm 1: TSA-SPA Algorithm

INPUT: Matrix $\boldsymbol{A}$, $\boldsymbol{A}_p \equiv (\partial \boldsymbol{A}/\partial p)$, shift point σ, eigenvalue estimate s_0, reduced matrix dimension k, number of computed eigenvalues l and tolerance ε

OUTPUT: Most sensitive eigenvalue λ_i and the corresponding eigenvectors $\boldsymbol{x}_i$ and $\boldsymbol{y}_i$, $i = 1, \ldots, l$

1> Execute TSA algorithm to generate $\boldsymbol{V}_k$, $\boldsymbol{W}_k$ and set $\boldsymbol{U}_k = \boldsymbol{W}_k^* \boldsymbol{V}_k$, $\boldsymbol{N}_k = \boldsymbol{W}_k^* \boldsymbol{A} \boldsymbol{V}_k$

2> Compute matrix $\boldsymbol{N}_p = \boldsymbol{W}_k^* \boldsymbol{A}_p \boldsymbol{V}_k$

3> Set $m = 0$ and $i = 0$, $\boldsymbol{v}_{r0}, \boldsymbol{w}_{r0} \in \Re^k$ s.t. $\boldsymbol{N}_p \boldsymbol{v}_{r0} \neq 0$ and $\boldsymbol{N}_p^* \boldsymbol{w}_{r0} \neq 0$

4> **while** $i < l$ **do**

5> **while** not converge **do**

a. $\boldsymbol{b}_r = \boldsymbol{N}_p \boldsymbol{v}_{rm} \Big/ \left\| \boldsymbol{N}_p \boldsymbol{v}_{rm} \right\|_2$

b. $\boldsymbol{c}_r = \boldsymbol{N}_p^* \boldsymbol{w}_{rm} \Big/ \left\| \boldsymbol{N}_p^* \boldsymbol{w}_{rm} \right\|_2$

c. Calculate $\boldsymbol{v}_{rm+1} \in \mathbb{C}^k$ from $(s_m \boldsymbol{U}_k - \boldsymbol{N}_k)\boldsymbol{v}_{rm+1} = \boldsymbol{b}_r$

d. Calculate $\boldsymbol{w}_{rm+1} \in \mathbb{C}^k$ from $(s_m \boldsymbol{U}_k - \boldsymbol{N}_k)^* \boldsymbol{w}_{rm+1} = \boldsymbol{c}_r$

e. Renew eigenvalue $s_{m+1} = \dfrac{\boldsymbol{w}_{rm+1}^* \boldsymbol{N}_k \boldsymbol{v}_{rm+1}}{\boldsymbol{w}_{rm+1}^* \boldsymbol{U}_k \boldsymbol{v}_{rm+1}}$

f. $\boldsymbol{x}_{ri} = \boldsymbol{v}_{rm+1} \Big/ \left\| \boldsymbol{v}_{rm+1} \right\|_2$ and $\boldsymbol{y}_{ri} = \boldsymbol{w}_{rm+1} \Big/ \left\| \boldsymbol{w}_{rm+1} \right\|_2$

g. If $\left\| \boldsymbol{N}_k \boldsymbol{x}_{ri} - s_{m+1} \boldsymbol{U}_k \boldsymbol{x}_{ri} \right\|_2 < \varepsilon$, then $i = i + 1$ and eigenvalue of matrix $\boldsymbol{N}_k$ is $\lambda_i = s_{m+1}$, compute the eigenvectors $\boldsymbol{x}_i = \boldsymbol{V}_k \boldsymbol{x}_{ri}$ and $\boldsymbol{y}_i = \boldsymbol{W}_k \boldsymbol{y}_{ri}$; λ_i is eigenvalue of Matrix $\boldsymbol{A}$, once it satisfies $\left\| \boldsymbol{A}\boldsymbol{x}_i - \lambda_i \boldsymbol{x}_i \right\|_2 < \varepsilon$ or $\left\| \boldsymbol{A}^* \boldsymbol{y}_i - \lambda_i^* \boldsymbol{y}_i \right\|_2 < \varepsilon$

h. Set $m = m + 1$

6> **end while**

7> Compute the matrix $\boldsymbol{T}_i = \frac{1}{\boldsymbol{y}_i^* \boldsymbol{x}_i} \boldsymbol{x}_i \boldsymbol{y}_i^*$,

8> Compute the matrix $\boldsymbol{T}_i = \boldsymbol{I} - \boldsymbol{T}_i$

9> Update sensitivity index $\boldsymbol{A}_p = \boldsymbol{T}_i \boldsymbol{A}_p \boldsymbol{T}_i$

10> Compute the matrix $\boldsymbol{N}_p = \boldsymbol{W}_k^* \boldsymbol{A}_p \boldsymbol{V}_k$

11> **end while**

B. Deflation Methods

Deflation methods are used to modify a matrix to eliminate the influence of a given eigenvector so that new eigenvalues other than the corresponding eigenvalue can be found sequentially. Widely-used deflation methods are reviewed in this section.

Wielandt deflation method [20] is one of the most effective methods for modifying the converged eigenvalue, which has been found to be less dominant (smaller in amplitude) and then continuing to compute other dominant eigenvalues. In the computation process, knowledge of only the converged right eigenvector $\boldsymbol{x}_i$ is required. The deflated matrix is of the form

$$\boldsymbol{A}_i = \boldsymbol{A} - \rho \boldsymbol{x}_i \boldsymbol{v}^* \tag{8}$$

where $\boldsymbol{v}$ is an arbitrary vector such that $\boldsymbol{v}^* \boldsymbol{x}_j = 1$, and ρ is an appropriate shift. The eigenvalues of $\boldsymbol{A}_i$ are the same as those of $\boldsymbol{A}$ except for eigenvalue λ_i which is transformed into eigenvalue $\lambda_i - \rho$. One of the most common choices is to set $\boldsymbol{v} = \boldsymbol{y}_i$ where $\boldsymbol{y}_i$ is the converged left eigenvector. This is referred to as Hotelling's deflation [20]. It can be proved that the choice $\boldsymbol{v} = \boldsymbol{x}_i$ can achieve an optimal result.

STEPS [17] adopted a deflation method described in [25]. It was used in conjunction with the inverse power method for sequential computation of the complete eigentriples in a specified study zone. The component in the direction of the known eigenvector is removed from the new eigenvector, which ensures that the found eigenvalue will not be obtained again.

An effective deflation method reported in [26] is proposed to realize multiple computation of sensitive eigenvalues in SASPA. The original matrix $\boldsymbol{A}$ is updated once the converged eigentriple is obtained, as shown below:

$$\boldsymbol{A}_j = \prod_j \left(\boldsymbol{I} - \frac{\boldsymbol{x}_j \boldsymbol{y}_j^*}{\boldsymbol{y}_j^* \boldsymbol{x}_j} \right) \boldsymbol{A} \prod_j \left(\boldsymbol{I} - \frac{\boldsymbol{x}_j \boldsymbol{y}_j^*}{\boldsymbol{y}_j^* \boldsymbol{x}_j} \right) \tag{9}$$

The renewed matrix $\boldsymbol{A}_j$ has the same eigentriples as matrix $\boldsymbol{A}$ but with the found eigenvalues transformed into zero. Two subspaces are then expanded with $\prod_j \left(\boldsymbol{I} - \frac{\boldsymbol{x}_j \boldsymbol{y}_j^*}{\boldsymbol{y}_j^* \boldsymbol{x}_j} \right) \boldsymbol{x}$ and $\prod_j \left(\boldsymbol{I} - \frac{\boldsymbol{x}_j \boldsymbol{y}_j^*}{\boldsymbol{y}_j^* \boldsymbol{x}_j} \right) \boldsymbol{y}$, respectively, where $\boldsymbol{x}$ and $\boldsymbol{y}$ are the iterative vectors.

III. GENERALIZED TSA-SPA METHOD

Equation (1) in Section II represents a general model of the dynamic system. A power system has numerous components so it is normally represented by a set of differential equations together with a set of algebraic equations [22]. The Jacobian matrix of the entire set of equations, at an operating point (x_0, y_0), can be rewritten as

$$\begin{bmatrix}\Delta\dot{\boldsymbol{X}}\\ \mathbf{0}\end{bmatrix}=\begin{bmatrix}\boldsymbol{J}_1 & \boldsymbol{J}_2\\ \boldsymbol{J}_3 & \boldsymbol{J}_4\end{bmatrix}\begin{bmatrix}\Delta\boldsymbol{X}\\ \Delta\boldsymbol{Y}\end{bmatrix} \quad (10)$$

where $\boldsymbol{X}$ denotes state variables of differential equations; $\boldsymbol{Y}$ denotes the algebraic variables $\boldsymbol{J}_1$, $\boldsymbol{J}_2$, $\boldsymbol{J}_3$ and $\boldsymbol{J}_4$ are the sub-matrices of the sparse Jacobian matrix applicable for large-scale systems' analysis. The power system state matrix can be obtained by eliminating the equations for algebraic variables in the Jacobian matrix:

$$\Delta\dot{\boldsymbol{X}}=\left(\boldsymbol{J}_1-\boldsymbol{J}_2\boldsymbol{J}_4^{-1}\boldsymbol{J}_3\right)\Delta\boldsymbol{X}=\boldsymbol{A}\Delta\boldsymbol{X} \quad (11)$$

A major drawback of state matrix $\boldsymbol{A}$ is lack of sparsity. As described in [22], state matrix $\boldsymbol{A}$ need not be fully formed when adopting the Arnoldi method for obtaining the reduced matrix $\boldsymbol{H}_k$. Since TSA inherits the advantage of Arnoldi method that can exploit sparsity effectively, therefore, for the generalized TSA-SPA method, the state matrix $\boldsymbol{A}$ also need not be fully formed for getting the perturbation matrix $\boldsymbol{A}_p\equiv\partial\boldsymbol{A}/\partial p$ ($\partial\boldsymbol{A}/\partial p$ is calculated by perturbation method $\Delta\boldsymbol{A}/\Delta p$). Instead, matrix $\boldsymbol{A}$ and $\Delta\boldsymbol{A}$ are reduced to $\boldsymbol{H}_k$ and $\Delta\boldsymbol{H}_k$ respectively, a much smaller scale, by using TSA, maintaining the good linear relationship between $\Delta\lambda$ and $\Delta\boldsymbol{H}_k$, as described in detail below.

A. Eigenvalue Computation

In TSA-SPA, forming the perturbation matrix $\boldsymbol{A}_p$ is inevitable for calculating the most sensitive eigenvalues. For changes of control parameters, the perturbed elements are all in the sub-matrix $\boldsymbol{J}_1$ of the Jacobian matrix, therefore, $\boldsymbol{A}_p$ is still sparse due to $\Delta\boldsymbol{J}_4=0$. However, for the changes of other system parameters such as power transfer, large numbers of elements in sub-matrix $\boldsymbol{J}_4$ vary, making heavy computational costs unavoidable for formation of the state matrix $\boldsymbol{A}$ and consequently matrix $\boldsymbol{A}_p$. Since state matrix $\boldsymbol{A}$ is dense, it is highly possible for $\boldsymbol{A}_p$ to be dense as well. Losing sparsity is undesirable, as a dense matrix often occupies large storage space in random access memory (RAM) and increases computation cost.

To solve the problem, a generalized TSA-SPA is proposed. According to the Arnoldi/TSA method [21], the following equation can be obtained by applying a small perturbation to (5).

$$(\boldsymbol{A}+\Delta\boldsymbol{A})(\boldsymbol{V}_k+\Delta\boldsymbol{V}_k)=(\boldsymbol{V}_k+\Delta\boldsymbol{V}_k)(\boldsymbol{H}_k+\Delta\boldsymbol{H}_k) \quad (12)$$

where for the sake of conciseness, all definitions of symbols are the same as in Section II; $\Delta\boldsymbol{A}$ is the abbreviation of $\boldsymbol{A}_p\Delta p$; $\Delta\boldsymbol{H}_k$ is the reduced matrix of $\Delta\boldsymbol{A}$ and is calculated by $\Delta\boldsymbol{H}_k=\boldsymbol{H}_k'-\boldsymbol{H}_k$, where $\boldsymbol{H}_k'$ denotes $\boldsymbol{H}_k$ after perturbation. Neglecting the perturbation's quadratic terms, (12) can be expressed as

$$\boldsymbol{A}\Delta\boldsymbol{V}_k+\Delta\boldsymbol{A}\boldsymbol{V}_k=\boldsymbol{V}_k\Delta\boldsymbol{H}_k+\Delta\boldsymbol{V}_k\boldsymbol{H}_k \quad (13)$$

Pre-multiplying $\boldsymbol{x}_r$ and post-multiplying $\boldsymbol{y}^*$ to (13),

$$\boldsymbol{y}^*\boldsymbol{A}\Delta\boldsymbol{V}_k\boldsymbol{x}_r+\boldsymbol{y}^*\Delta\boldsymbol{A}\boldsymbol{V}_k\boldsymbol{x}_r=\boldsymbol{y}^*\boldsymbol{V}_k\Delta\boldsymbol{H}_k\boldsymbol{x}_r+\boldsymbol{y}^*\Delta\boldsymbol{V}_k\boldsymbol{H}_k\boldsymbol{x}_r \quad (14)$$

Since $\boldsymbol{y}^*\boldsymbol{A}=\boldsymbol{\lambda}\boldsymbol{y}^*$, $\boldsymbol{V}_k\boldsymbol{x}_r=\boldsymbol{x}$ and $\boldsymbol{H}_k\boldsymbol{x}_r=\boldsymbol{\lambda}\boldsymbol{x}_r$, it can be deduced that

$$\boldsymbol{y}^*\Delta\boldsymbol{A}\boldsymbol{x}=\boldsymbol{y}^*\boldsymbol{V}_k\Delta\boldsymbol{H}_k\boldsymbol{x}_r \quad (15)$$

Based on the definition of sensitivity of eigenvalues equation (4), (15) can be written as

$$\Delta\lambda/\Delta p=\boldsymbol{y}_r^*\boldsymbol{U}_k\Delta\boldsymbol{H}_k\boldsymbol{x}_r \quad (16)$$

where $\boldsymbol{U_k}=\boldsymbol{W}_k^*\boldsymbol{V}_k$, Similarly, based on $\boldsymbol{y}^*=\boldsymbol{y}_r^*\boldsymbol{W}_k^*$, the sensitivity of eigenvalues can be calculated by

$$\Delta\lambda/\Delta p=\boldsymbol{y}_r^*\Delta\boldsymbol{M}_k^*\boldsymbol{U}_k\boldsymbol{x}_r \quad (17)$$

It can be readily seen that the sensitivity can be calculated in the matrices with reduced dimension, and computation of the perturbation matrix $\boldsymbol{A}_p$ is avoided and replaced successfully by reduced matrices. From equations (16) and (17), it can be seen that if the relationships are built as $\boldsymbol{b}=\Delta\boldsymbol{H}_k\boldsymbol{x}_{ri}$ and $\boldsymbol{c}=\Delta\boldsymbol{M}_k\boldsymbol{y}_{ri}$, then the eigenvalue with the largest residue of the reduced matrix $\boldsymbol{W}_k^*\boldsymbol{A}\boldsymbol{V}_k$ is:

$$\begin{aligned}R_i&=(\boldsymbol{c}^*\boldsymbol{U}_k\boldsymbol{x}_{ri})(\boldsymbol{y}_{ri}^*\boldsymbol{U}_k\boldsymbol{b})\\&=(\boldsymbol{y}_{ri}^*\Delta\boldsymbol{M}_k^*\boldsymbol{U}_k\boldsymbol{x}_{ri})(\boldsymbol{y}_{ri}^*\boldsymbol{U}_k\Delta\boldsymbol{H}_k\boldsymbol{x}_{ri})\\&=(\boldsymbol{y}_i^*\frac{\partial\boldsymbol{A}}{\partial\boldsymbol{p}}\boldsymbol{x}_i)^2=(\frac{\partial\lambda_i}{\partial p})^2\end{aligned} \quad (18)$$

The largest residue R_i accords with the one obtained by SPA. Therefore, similar to TSA-SPA, the generalized TSA-SPA algorithm can also compute the most sensitive eigentriples. During iterations, vectors $\boldsymbol{b}$ and $\boldsymbol{c}$ are renewed by the right and left eigenvectors $\boldsymbol{x}_{ri}$ and $\boldsymbol{y}_{ri}$ with pre-multiplication with matrix $\boldsymbol{U}_k\Delta\boldsymbol{H}_k$ and $\boldsymbol{U}_k\Delta\boldsymbol{M}_k$ respectively, until eigenvectors $\boldsymbol{x}_{ri}$ or $\boldsymbol{y}_{ri}$ converge.

It is noted that when precondition transformation is adopted, i.e. shift-invert transformation in this paper, the largest residue of (18) no longer equals to $(\frac{\partial\lambda_i}{\partial p})^2$. Assume the eigenvalue λ_i becomes λ_i' after perturbation and the sensitivity of the eigenvalue $\frac{\partial\lambda_i}{\partial p}$ can be approximated by $\frac{\lambda_i'-\lambda_i}{\Delta p}$. It can be easily proved that the eigenvalue's sensitivity of the reduced matrix is $\frac{\lambda_i'-\lambda_i}{(\lambda_i'-\sigma)(\lambda_i-\sigma)\Delta p}$. To correct the sensitivity of eigenvalues of the reduced matrix, $\Delta\boldsymbol{H}_k$ should be calculated by $\Delta\boldsymbol{H}_k=\boldsymbol{H}_k'^{-1}-\boldsymbol{H}_k^{-1}$, and $\Delta\boldsymbol{M}_k=\boldsymbol{M}_k'^{-1}-\boldsymbol{M}_k^{-1}$, where $\boldsymbol{M}_k'$ denote $\boldsymbol{M}_k$ after perturbation.

The procedure of the proposed algorithm is shown in Alg. 2. Similar to the TSA-SPA, the initial eigen-problem is reduced to $(\boldsymbol{N}_k,\boldsymbol{U}_k)$ by using TSA at first, and then the most sensitive eigenvalues are calculated from $(\boldsymbol{N}_k,\boldsymbol{U}_k)$ by SPA. Different from the TSA-SPA, $\Delta\boldsymbol{A}$ is reduced to $\Delta\boldsymbol{H}_k$ and $\Delta\boldsymbol{M}_k$ by TSA. The main advantage is that the sparsity technique can be still applied in the proposed algorithm. Besides, during iteration, vectors renewed at Steps 4a~4d have only dimension of k, where $k<<n$, thus it has small computation cost. Moreover, similar to TSA-SPA, shift-invert transformation can also be realized in Step 1 for building the two Krylov subspaces $\boldsymbol{V}_k$ and $\boldsymbol{W}_k$; thus $(\boldsymbol{N}_k,\boldsymbol{U}_k)$ usually contains several eigenvalues around the given shift point. Finally, with the deflation procedure, the proposed algorithm can readily calculate several other sensitive eigenvalues.

Algorithm 2: Generalized TSA-SPA Algorithm

INPUT: Jacobian Matrix $\boldsymbol{J}$, Jacobian matrix under perturbation $\boldsymbol{J}'$, shift point σ, eigenvalue estimate s_0, reduced matrix dimension k, number of computed eigenvalues l and tolerance ε

OUTPUT: Most sensitive eigenvalue λ_i and corresponding eigenvectors $\boldsymbol{x}_i$ and $\boldsymbol{y}_i$

1> Execute TSA algorithm to Jacobian matrix $\boldsymbol{J}$ to generate $\boldsymbol{V}_k$, $\boldsymbol{W}_k$ and set $\boldsymbol{U}_k = \boldsymbol{W}_k^* \boldsymbol{V}_k$, $\boldsymbol{N}_k = \boldsymbol{W}_k^* \boldsymbol{A} \boldsymbol{V}_k$

2> Execute TSA algorithm to Jacobian matrix under perturbation $\boldsymbol{J}'$ to generate matrix $\Delta \boldsymbol{H}_k$ and $\Delta \boldsymbol{M}_k$

3> Set $m=0$ and $i=0$, $\boldsymbol{v}_{r0}, \boldsymbol{w}_{r0} \in \Re^k$ s.t. $\Delta \boldsymbol{H}_k \boldsymbol{v}_{r0} \neq 0$ and $\Delta \boldsymbol{M}_k \boldsymbol{w}_{r0} \neq \boldsymbol{0}$

4> **while** not converge **do**

a. $\boldsymbol{b}_r = \Delta \boldsymbol{H}_k \boldsymbol{v}_{rm} / \|\Delta \boldsymbol{H}_k \boldsymbol{v}_{rm}\|_2$

b. $\boldsymbol{c}_r = \Delta \boldsymbol{M}_k \boldsymbol{w}_{rm} / \left\|\Delta \boldsymbol{M}_k \boldsymbol{w}_{rm}\right\|_2$

c. Calculate $\boldsymbol{v}_{rm+1} \in \mathbb{C}^k$ from $(s_m \boldsymbol{U}_k - \boldsymbol{N}_k)\boldsymbol{v}_{rm+1} = \boldsymbol{U}_k \boldsymbol{b}_r$

d. Calculate $\boldsymbol{w}_{rm+1} \in \mathbb{C}^k$ from $(s_m \boldsymbol{U}_k - \boldsymbol{N}_k)^* \boldsymbol{w}_{rm+1} = \boldsymbol{U}_k^* \boldsymbol{c}_r$

e. Renew eigenvalue $s_{m+1} = \dfrac{\boldsymbol{w}_{rm+1}^* \boldsymbol{N}_k \boldsymbol{v}_{rm+1}}{\boldsymbol{w}_{rm+1}^* \boldsymbol{U}_k \boldsymbol{v}_{rm+1}}$

f. $\boldsymbol{x}_{ri} = \boldsymbol{v}_{rm+1} / \|\boldsymbol{v}_{rm+1}\|_2$ and $\boldsymbol{y}_{ri} = \boldsymbol{w}_{rm+1} / \|\boldsymbol{w}_{rm+1}\|_2$

g. If $\|\boldsymbol{N}_k \boldsymbol{x}_{ri} - s_{m+1} \boldsymbol{U}_k \boldsymbol{x}_{ri}\|_2 < \varepsilon$, then $i=i+1$ and eigenvalue of matrix $\boldsymbol{N}_k$ is $\lambda_i = s_{m+1}$, compute the eigenvectors $\boldsymbol{x}_i = \boldsymbol{V}_k \boldsymbol{x}_{ri}$ and $\boldsymbol{y}_i = \boldsymbol{W}_k \boldsymbol{y}_{ri}$; λ_i is eigenvalue of Matrix $\boldsymbol{A}$, once it satisfies $\left\|\boldsymbol{A}\boldsymbol{x}_i - \lambda_i \boldsymbol{x}_i\right\|_2 < \varepsilon$ or $\left\|\boldsymbol{A}^* \boldsymbol{y}_i - \lambda_i^* \boldsymbol{y}_i\right\|_2 < \varepsilon$

h. Set $m=m+1$

5> **end while**

B. New Deflation Method

The available deflation methods discussed in Section II.B cannot be directly applied to the proposed algorithm. Deflation methods of Wielandt, Hotelling and one adopted in STEPS fail to eliminate the influence of both right and left converged eigenvectors simultaneously, which leads to the change of sensitivity of eigenvalues in the deflation process. The deflation method proposed in SASPA is effective and reliable for finding several distinct sensitive eigenvalues but the deflation is applied to state matrix $\boldsymbol{A}$ and thus has high computation cost for large systems. For the deflation method proposed in TSA-SPA, the perturbation matrix $\boldsymbol{A}_p$ is essential and it is no longer available in the proposed algorithm in this paper. To realize computation of several distinct sensitive eigenvalues in the reduced matrix, an effective deflation method in conjunction with the generalized TSA-SPA is proposed, as shown in Alg. 3. For finding the several sensitive eigenvalues, just modifying the obtained eigenvalues' amplitude is insufficient. At the same time, inappropriate elimination of the given eigenvector may induce large sensitivity to the associated eigenvalues. The main advantage of the proposed deflation method is that once an eigenvalue is obtained, it is no longer dominant (not sensitive) in the deflation procedure. Different from deflation method proposed in [26, 27], the deflation procedure calculates all the sensitive eigenvalues in the same reduced matrix $\boldsymbol{N}_k$ and no additional renewal of the subspace is needed (see Step 4e and Step 4f in Alg. 3). Following this deflation method, a continued multiplication of the correct factor matrix for the iterative vector is adopted for better rounding off error elimination (see Step 3 in Alg. 3).

It is essential to prove that the iterative Steps 4a and 4b can effectively avoid the repeated convergence to the same converged eigenvectors while sensitivities of other eigenvalues are not changed. Thus, two cases are discussed separately:

1> $\boldsymbol{v}_{rm}$ converges to the same eigenvector as in previous iterations, i.e. $\boldsymbol{v}_{rm} \to \boldsymbol{x}_{ri}$; In this case, the iterative vector can be written as (for the sake of conciseness, only the iterative vector $\boldsymbol{b}_r$ is adopted in the proof, the continuous multiplication is also omitted since the proof is similar):

$$\boldsymbol{b}_r = \left(\boldsymbol{I} - \frac{\boldsymbol{x}_{ri} \boldsymbol{y}_{ri}^* \boldsymbol{U}_k}{\boldsymbol{y}_{ri}^* \boldsymbol{U}_k \boldsymbol{x}_{ri}}\right) \Delta \boldsymbol{H}_k \boldsymbol{x}_{ri}$$

Thus, from Equation (18), the right part of residue index R_i, $\boldsymbol{y}_{ri}^* \boldsymbol{U}_k \boldsymbol{b}_r$ can be written as:

$$\begin{aligned} &\boldsymbol{y}_{ri}^* \boldsymbol{U}_k \boldsymbol{b}_r \\ &= \left(\boldsymbol{y}_{ri}^* \boldsymbol{U}_k \Delta \boldsymbol{H}_k \boldsymbol{x}_{ri} - \boldsymbol{y}_{ri}^* \boldsymbol{U}_k \frac{\boldsymbol{x}_{ri} \boldsymbol{y}_{ri}^* \boldsymbol{U}_k \Delta \boldsymbol{H}_k \boldsymbol{x}_{ri}}{\boldsymbol{y}_{ri}^* \boldsymbol{U}_k \boldsymbol{x}_{ri}}\right) \\ &= \left(\frac{\partial \boldsymbol{\lambda}}{\partial \boldsymbol{p}} - \boldsymbol{y}_{ri}^* \boldsymbol{U}_k \boldsymbol{x}_{ri} \frac{\frac{\partial \boldsymbol{\lambda}}{\partial \boldsymbol{p}}}{\boldsymbol{y}_{ri}^* \boldsymbol{U}_k \boldsymbol{x}_{ri}}\right) = 0 \end{aligned}$$

Therefore, the iterative vector can never converge to the same converged eigenvectors since the residue index is eliminated and is zero; in other words, the sensitivity of the pre-converged eigenvalue is reduced to zero. Furthermore, with the continuous multiplication of the correct factor matrix, any convergence to the previously converged eigenvectors is avoided successfully.

2> $\boldsymbol{v}_{rm}$ converges to a new eigenvector $\boldsymbol{x}_{rj}$. In this case, the iterative vector can be written as :

$$\boldsymbol{b}_r = \left(\boldsymbol{I} - \frac{\boldsymbol{x}_{ri} \boldsymbol{y}_{ri}^* \boldsymbol{U}_k}{\boldsymbol{y}_{ri}^* \boldsymbol{U}_k \boldsymbol{x}_{ri}}\right) \Delta \boldsymbol{H}_k \boldsymbol{x}_{rj} \tag{19}$$

Similar to Case 1, the right part of residue index R_i, $\boldsymbol{y}_{rj}^* \boldsymbol{U}_k \boldsymbol{b}_r$ can be written as:

$$\boldsymbol{y}_{rj}^* \boldsymbol{U}_k \boldsymbol{b}_r = \boldsymbol{y}_{rj}^* \boldsymbol{U}_k \Delta \boldsymbol{H}_k \boldsymbol{x}_{rj} - \frac{\boldsymbol{y}_{rj}^* \boldsymbol{U}_k \boldsymbol{x}_{ri} \boldsymbol{y}_{ri}^* \boldsymbol{U}_k}{\boldsymbol{y}_{ri}^* \boldsymbol{U}_k \boldsymbol{x}_{ri}} \Delta \boldsymbol{H}_k \boldsymbol{x}_{rj}$$

It is easy to prove that numerator of the second item of the above equation $\boldsymbol{y}_{rj}^* \boldsymbol{U}_k \boldsymbol{x}_{ri} \equiv 0$. Therefore, the second item of the above equation equals to zero. As a consequence, the relationship is the same as Equation (12). In other words, the residue index remains

unchanged. Thus the iterative vector keeps the sensitivity of eigenvalues unchanged and therefore, it is guaranteed that other sensitive eigenvalues can be found in the iterations.

From the point of view of implementation, Steps 2 and 3 of Alg. 2 do not need to be formed explicitly. The only operation required is matrix-vector operation in small scale. More specifically, the update of vectors (Step 2 and Step 3 of Alg. 2) can be incorporated in Step 4a, as shown in Alg. 4, the vector $\boldsymbol{b}_r$, for example, can be formed, where $\boldsymbol{x}_{ri}$and $\boldsymbol{y}_{\boldsymbol{ri}}$denote the converged eigenvector corresponding to λ_i, respectively.

Algorithm 3: Deflation in TSA-SPA

INPUT: $\boldsymbol{X} = \{\boldsymbol{x}_{r1}, \dots, \boldsymbol{x}_{rk}\}$ with $\boldsymbol{X}^*\boldsymbol{X} = \boldsymbol{I}$, satisfying $\boldsymbol{A}\boldsymbol{V}_k\boldsymbol{x}_{ri} = \lambda_i\boldsymbol{V}_k\boldsymbol{x}_{ri}$; $\boldsymbol{Y} = \{\boldsymbol{y}_{r1}, \dots, \boldsymbol{y}_{rk}\}$ with $\boldsymbol{Y}^*\boldsymbol{Y} = \boldsymbol{I}$, satisfying $\boldsymbol{A}^*\boldsymbol{W}_k\boldsymbol{y}_{ri} = \lambda_i^*\boldsymbol{W}_k\boldsymbol{y}_{ri}$, $i = 1, \dots, k$ and number of computed eigenvalues l

OUTPUT: Most sensitive eigenvalue λ_j and corresponding eigenvectors $\boldsymbol{x}_j$ and $\boldsymbol{y}_j$, $j = k+1, \dots, l; i = 1, \dots, l$

1> Set $\boldsymbol{v}_{r0}, \boldsymbol{w}_{r0} \in \Re^k$ s.t. $\Delta\boldsymbol{H}_k\boldsymbol{v}_{r0} \neq 0$ and $\Delta\boldsymbol{M}_k\,\boldsymbol{w}_{\boldsymbol{r0}} \neq \boldsymbol{0}$

2> Form the correct factor matrix $\boldsymbol{I} - \frac{\boldsymbol{x}_{ri}\boldsymbol{y}_{ri}^*\boldsymbol{U}_k}{\boldsymbol{y}_{ri}^*\boldsymbol{U}_k\boldsymbol{x}_{ri}}$, $i = 1, \dots, k$

3> Form the matrix $\prod_{i=1}^{k}\left(\boldsymbol{I} - \frac{\boldsymbol{x}_{ri}\boldsymbol{y}_{ri}^*\boldsymbol{U}_k}{\boldsymbol{y}_{ri}^*\boldsymbol{U}_k\boldsymbol{x}_{ri}}\right)$

4> **while** not converge **do**

a. $\boldsymbol{b}_r = \prod_{i=1}^{k}\left(\boldsymbol{I} - \frac{\boldsymbol{x}_{ri}\boldsymbol{y}_{ri}^*\boldsymbol{U}_k}{\boldsymbol{y}_{ri}^*\boldsymbol{U}_k\boldsymbol{x}_{ri}}\right)\Delta\boldsymbol{H}_k\boldsymbol{v}_{rm}$

b. $\boldsymbol{b}_r = \boldsymbol{b}_r/\|\boldsymbol{b}_r\|_2$

c. $\boldsymbol{c}_r = \prod_{i=1}^{k}\left(\boldsymbol{I} - \frac{\boldsymbol{y}_{ri}\boldsymbol{x}_{ri}^*\boldsymbol{U}_k^*}{\boldsymbol{x}_{ri}^*\boldsymbol{U}_k^*\boldsymbol{y}_{ri}}\right)\Delta\boldsymbol{M}_k\,\boldsymbol{w}_{rm}$

d. $\boldsymbol{c}_r = \boldsymbol{c}_r/\|\boldsymbol{c}_r\|_2$

e. Calculate $\boldsymbol{v}_{rm+1} \in \mathbb{C}^k$ from $(s_m\boldsymbol{U}_k - \boldsymbol{N}_k)\boldsymbol{v}_{rm+1} = \boldsymbol{U}_k\boldsymbol{b}_r$

f. Calculate$\boldsymbol{w}_{rm+1} \in \mathbb{C}^k$from $(s_m\boldsymbol{U}_k - \boldsymbol{N}_k)^*\boldsymbol{w}_{rm+1} = \boldsymbol{U}_k^*\boldsymbol{c}_r$

g. Renew eigenvalue $s_{m+1} = \frac{\boldsymbol{w}_{rm+1}^*\boldsymbol{N}_k\boldsymbol{v}_{rm+1}}{\boldsymbol{w}_{rm+1}^*\boldsymbol{U}_k\boldsymbol{v}_{rm+1}}$

h. $\boldsymbol{x}_{ri} = \boldsymbol{v}_{rm+1}/\|\boldsymbol{v}_{rm+1}\|_2$ and $\boldsymbol{y}_{ri} = \boldsymbol{w}_{rm+1}/\|\boldsymbol{w}_{rm+1}\|_2$

i. If $\|\boldsymbol{N}_k\boldsymbol{x}_{ri} - s_{m+1}\boldsymbol{U}_k\boldsymbol{x}_{ri}\|_2 < \varepsilon$, then eigenvalue of matrix $\boldsymbol{N}_k$ is $\lambda_i = s_{m+1}$, compute the eigenvectors $\boldsymbol{x}_i = \boldsymbol{V}_k\boldsymbol{x}_{ri}$ and $\boldsymbol{y}_i = \boldsymbol{W}_k\boldsymbol{y}_{ri}$;λ_i is eigenvalue of Matrix $\boldsymbol{A}$, once it satisfies $\|\boldsymbol{A}\boldsymbol{x}_i - \lambda_i\boldsymbol{x}_i\|_2 < \varepsilon$ or $\|\boldsymbol{A}^*\boldsymbol{y}_i - \lambda_i{}^*\boldsymbol{y}_i\|_2 < \varepsilon$

j. Set $m = m + 1$

5> **end while**

Algorithm 4: Update vectors in deflation method

INPUT: $\boldsymbol{v}_{rm}$, $\Delta\boldsymbol{H}_k$, $\boldsymbol{x}_{ri}$, $\boldsymbol{y}_{\boldsymbol{ri}}$

OUTPUT: $\boldsymbol{b}_r$

1> $\boldsymbol{v}_{rm} = \Delta\boldsymbol{H}_k\boldsymbol{v}_{rm}$

2> **do** $i = k,\ 1,\ -1$

a. $\boldsymbol{v}_{rm} = \boldsymbol{U}_k\boldsymbol{v}_{rm}$; $\boldsymbol{v}_{tmp} = \boldsymbol{U}_k\boldsymbol{x}_{ri}$

b. $\boldsymbol{v}_{r_{tmp}} = \frac{(\boldsymbol{y}_{ri}, \boldsymbol{v}_r)}{(\boldsymbol{y}_{ri}, \boldsymbol{v}_{tmp})} * \boldsymbol{x}_{ri}$

c. $\boldsymbol{v}_{\boldsymbol{rm}} = \boldsymbol{v}_{\boldsymbol{rm}} - \boldsymbol{v}_{r_{tmp}}$

3> **end do**

4> $\boldsymbol{b}_r = \boldsymbol{v}_{\boldsymbol{rm}}$

IV. Simulation Results of A Small Power System

This section describes numerical results of application of the generalized TSA-SPA in the IEEE 9-bus system. Static and dynamic data of the system can be found from [21]. This paper studies four scenarios with perturbation on different parameters including (1) increasing K_{PSS} of PSS installed at Generator G_2; (2) increasing load at Bus 5; (3) increasing active power output at Generator G_2 and decreasing active power output at Generator G_3; and (4) decreasing reactance of Lines 7-8 and 8-9. Perturbation is set as 1% of the initial values. Sensitivity of eigenvalue is calculated by $\Delta\lambda_i/|\Delta\boldsymbol{p}|_2$, where $\Delta\lambda_i$ denotes the variation of sensitive eigenvalue λ_i under perturbation and $|\Delta\boldsymbol{p}|_2$ denotes the 2-norm of the perturbed parameter vector $\Delta\boldsymbol{p}$. The simulations were carried out on PC (3.16-GHz Intel Core Duo, 3.25GB usable RAM) and the program is written in Fortran 90. This system has 21 state variables. Size of Krylov subspace, reduced matrix dimension k, number of wanted eigenvalues l and tolerance ε are set to be 20, 8, 4 and 10^{-6}, respectively. Initial vectors are chosen as $\boldsymbol{v}_{r0} = \boldsymbol{w}_{r0} = [1, \dots, 1] \in R^k$ (cf. Step 3 of Alg. 2).

In this study, four sensitive eigenvalues are calculated for each scenario by the generalized TSA-SPA using deflation method, as shown in Tables I to IV. The shift point is selected as the point of damping ratio of 50% with frequency 2.0Hz, i.e., $\sigma = (-7.26,\ 12.57)$. The sensitivities and state variables with maximum participation factor (PF) for these eigenvalues are tabulated; δ_i, V_{Ri}, E'_{qi}, E'_{di} denote rotor angle, exciter input, q-axis and d-axis component of the voltage behind transient reactance of generator G_i, respectively.

Scenario 1 with the same conditions as in [21] is used to compare the performance of the generalized TSA-SPA with the TSA-SPA for control parameters' perturbation. Table I shows the calculated eigenvalues and the corresponding sensitivity are the same as reported in [21], up to four decimal places, which clearly illustrates that linearization of the reduced matrix under perturbation proposed in the generalized TSA-SPA has good approximation to the state matrix under perturbation. It does not affect the accuracy of TSA-SPA and can be extended to system parameters changes. Tables II, III and IV show that the generalized TSA-SPA can also successfully calculate the eigenvalues sensitive to the system operating parameters under Scenarios 2 and 3 and network parameters in Scenario 4, respectively. Accuracy of the results has been confirmed by complete eigenvalue computation using the QR method. For example, in Scenario 2, the six most sensitive eigenvalues and the corresponding sensitivity obtained by the QR method are listed in Table V. Compared to Table II, it is clear that the generalized TSA-SPA can selectively calculate sensitive eigenvalues. Scenario 2 is also used to illustrate the robustness of the generalized TSA-SPA. Eigenvalue estimate s_0 in Alg. 2 is varied in an arbitrarily given complex plane (Fig. 1). A symbol at point (x, y) in complex plane means that the

generalized TSA-SPA starts with an initial eigenvalue estimate $s_0 = x + jy$ and converges to the eigenvalue corresponding to the symbol in Table V. For any initial eigenvalue estimates, the method obtains the same sensitive eigenvalue (-0.6452 +j12.7459) and performs robustly.

Besides, the influence of the shift point σ on the calculated eigenvalues is also studied (Fig. 2). A symbol at point (x, y) in complex plane means the generalized TSA-SPA starts with a shift point $\sigma = x + jy$ and converges to the eigenvalue corresponding to the symbol in Table V. Symbol × in Fig. 2 denotes the less sensitive eigenvalues, i.e. eigenvalues not in the list (Table V). For the generalized TSA-SPA, shift point σ has great influence on eigenvalues computed, but the sensitive eigenvalues in a region can always be found with reasonable shift points. In other words, the shift points can be used to select the region to be studied, demonstrating the flexibility of the generalized TSA-SPA.

TABLE I
SENSITIVE EIGENVALUES FOR SCENARIO 1

Deflation number	Eigenvalue	Sensitivity	State variable with max PF
0	-5.8025 + j7.7888	-0.3131 – j0.1514	V_{R2}
1	-0.0339 + j8.5278	0.1482 + j0.1533	δ_2
2	-0.6452 + j12.7459	0.0741 – j0.0009	δ_3
3	-0.4487 + j1.1950	-0.0034 – j0.0145	E'_{q1}

TABLE II
SENSITIVE EIGENVALUES FOR SCENARIO 2

Deflation number	Eigenvalue	Sensitivity (10^{-1})	State variable with max PF
0	-0.6452 + j12.7459	-0.7081 – j0.7192	δ_3
1	-0.0339 + j8.5278	-0.4096 – j0.3112	δ_2
2	-5.1741	1.6090	E'_{d2}
3	-5.8025 + j7.7889	-0.4576 + j0.0848	V_{R2}

TABLE III
SENSITIVE EIGENVALUES FOR SCENARIO 3

Deflation number	Eigenvalue	Sensitivity (10^{-1})	State variable with max PF
0	-0.6452 + j12.7459	-0.1662 – j0.1624	δ_3
1	-5.1741	0.1901	E'_{d2}
2	-3.3997	0.1487	E'_{d3}
3	-5.8025 + j7.7889	-0.0511 + j0.0034	V_{R2}

TABLE IV
SENSITIVE EIGENVALUES FOR SCENARIO 4

Deflation number	Eigenvalue	Sensitivity	State variable with max. PF
0	-0.6452 + j12.7459	0.0212 + j0.2863	δ_3
1	-5.1741	-0.2154	E'_{d2}
2	-3.3997	0.0461	E'_{d3}
3	-0.4487 + j1.1949	0.0204 – j0.0331	E'_{q1}

TABLE V
SIX MOST SENSITIVE EIGENVALUES FOR SCENARIO 2 OBTAINED BY QR METHOD

No.	Eigenvalue (symbol)	Sensitivity (10^{-1})	State variable with max. PF
1	-5.1741 (Square ■)	1.6090	E'_{d2}
2	-0.6452 + j12.7459 (Dot ●)	-0.7081 – j0.7192	δ_2
3	-0.0339 + j8.5278 (Circle ○)	-0.4096 – j0.3112	δ_3
4	-3.3997 (Star ∗)	0.4950	E'_{d3}
5	-0.4487 + j1.1949 (Diamond ◆)	-0.0792 + j0.4844	E'_{q1}
6	-5.8025 + j7.7889 (Triangle ▲)	-0.4576 + j0.0848	V_{R2}

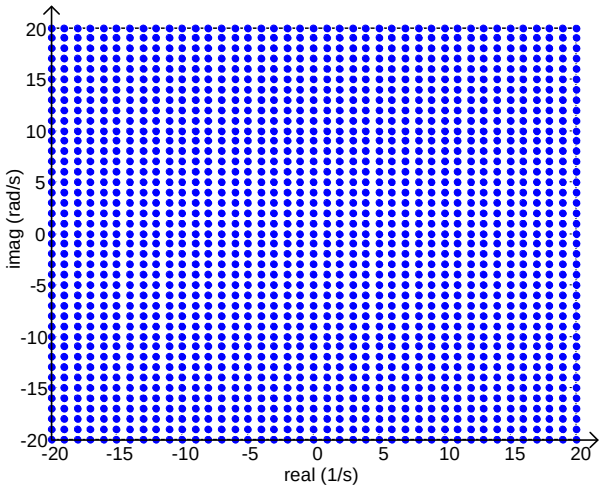

Fig. 1. Sensitive eigenvalue convergence areas for generalized TSA-SPA in the 9-bus system

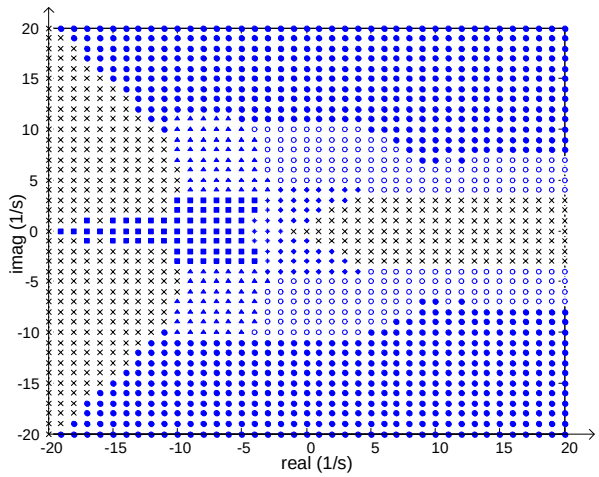

Fig. 2. Eigenvalues obtained by generalized TSA-SPA for different shift points in the 9-bus system

V. SIMULATION RESULTS OF LARGE-SCALE POWER SYSTEMS

In this section, the generalized TSA-SPA is applied in a large-scale power system, the entire eastern US-Canada interconnected system [28]. This system has 52 areas with 37587 state variables while the dimension of the augmented Jacobian matrix is 108331. Change of different types of parameters including control, system operating and system network parameters are studied. As low frequency oscillations often occur in weakly connected large-scale systems, sensitive eigenvalues of inter-area mode are the focus. The region of interest in the complex plane is set to have frequencies from 0.2Hz to 0.6Hz with damping ratios of 1% to 10%. Size of Krylov subspace and reduced matrix (k) are set to be 120 and

60, respectively. The simulation platform and other initial settings are same as the small power system in Section IV.

A. Change of Control Parameter

For performance comparison, the settings used for TSA-SPA in [21] are used for the generalized approach. The control parameters' perturbation in [21], the gain of a PSS at generator G_{87456}, is adopted. The shift points σ with damping ratio of 5% and frequency of 0.4Hz, i.e. (-0.1258, 2.5133), and with damping ratio of 5% and frequency of 1.7, i.e. (-0.5347, 10.6814) in [21] are also used for computation of inter-area and local modes, respectively. The proposed deflation method is used to sequentially compute the four highest sensitivity inter-area (i.e. l = 4) and three local modes (i.e. l = 3) as shown in Table VI and Table VII, respectively. Compared to the results shown in [21], sensitivities of eigenvalues obtained from generalized TSA-SPA have the same values up to four decimal places, which illustrates the generalized TSA-SPA keeps the powerful computational feature of TSA-SPA in the application of large-scale power systems.

B. Change of System Operating Parameter

For the system operating parameters' perturbation, generators' output variations at G_{10873} and G_{14924} are adopted. Implicitly Restarted Arnoldi Method (IRAM), which is widely used for eigenvalue analysis in large-scale system [21,22], is first adopted to calculate all eigenvalues in this region using different shift points. Totally 875 eigenvalues are obtained and the top ten sensitive eigenvalues are tabulated in Table VIII. When a shift point with damping ratio of 5% and frequency of 0.5Hz, i.e. (-0.0943, 3.1416), is assumed for the generalized TSA-SPA, the four highest sensitivity inter-area modes are successfully obtained sequentially by the deflation procedure shown in Table IX. The computing time is 329.1s. Besides, the influence of the change of eigenvalue estimate on calculated eigenvalues is also studied for the large-scale power system. Similar to the small power system in Section IV, the generalized TSA-SPA is also very robust to the eigenvalue estimate and the initial estimate will not affect the final result. Besides, the obtained eigenvalues of inter-area modes for different shift points are shown in Fig. 3. It is clear that the proposed method can selectively calculate these sensitive eigenvalues out of 875 eigenvalues locating in the region of interest.

C. Change of System Network Parameter

For the system network parameters' perturbation, reactance changes of the selected circuit from Bus_{10071} to Bus_{14923}, which is the part of the tie line between east and west regions with length approximately more than 300 km, is adopted. The perturbation parameter is the reactance of the selected circuit with the increase of 5%. Table X lists the top ten sensitive eigenvalues obtained by IRAM while Table XI provides the four sensitive inter-area modes obtained by the generalized TSA-SPA with the shift point (-0.0943, 3.1416). From the results, it can be seen that the generalized TSA-SPA can find the most sensitive eigenvalues around the shift with satisfactory reliability.

D.Accuracy Validation

The eigenvalue and the corresponding sensitivity calculated by the generalized TSA-SPA are compared with that obtained by IRAM. Therefore, the results in Tables VI and VII for control parameters study are compared with the results reported in [21] while the results in Tables IX and XI for system operating and network parameters are compared with Tables VIII and X, respectively. The relative error (RE) of eigenvalues and the corresponding sensitivities in different cases is summarized in Table XII. In all cases, the generalized TSA-SPA can achieve accurate results. It should be noted that the larger the sensitivity is, the less the relative error will be. For example, the RE of sensitive eigenvalue (-0.1261+j2.8236) is around 3% mainly due to its low sensitivity (Table VI), which is obtained in the second round of the deflection. In general, the RE of high eigenvalues and the corresponding sensitivities are less than 0.01% and 1.5%, respectively, in this large-scale power system, so the accuracy of the generalized TSA-SPA is satisfactory for practical application.

E. Discussion on Computational Performance

The computation cost in the above cases is as listed in Table XIII. In the Iteration column, the item in the summation denotes the number of iteration steps required for obtaining each sensitive eigenvalue. The first two items of the summation denote the number of iterations in n-dimension for building the right and left Krylov subspaces for a given size of reduced matrix. It is clear that the computation cost is nearly the same as the three kinds of parameter changes, but it increases with the increase of the Krylov subspace dimension. Simulation results also agree with the recommendation in [20] that the size of Krylov subspace being twice the reduced matrix is practically sufficient to guarantee convergence to good eigenvalue approximations.

In IRAM, $\boldsymbol{A}_p$ can be obtained by derivatives of sub-matrices of system Jacobian matrix in (10) with respect to system parameters, i.e. $\boldsymbol{A}_p = \dot{\boldsymbol{J}}_1 - \dot{\boldsymbol{J}}_2\boldsymbol{J}_4^{-1}\boldsymbol{J}_3 + \boldsymbol{J}_2\boldsymbol{J}_4^{-1}\dot{\boldsymbol{J}}_4\boldsymbol{J}_4^{-1}\boldsymbol{J}_3 - \boldsymbol{J}_2\boldsymbol{J}_4^{-1}\dot{\boldsymbol{J}}_3$, where $\dot{\boldsymbol{J}}_i$ denotes the derivative of sub-matrix $\boldsymbol{J}_i$ with respect to system parameters. Suppose $\boldsymbol{J}_4$ has dimension m, and $m>>n$, obviously the computation cost is high due to the multiple multiplications of the matrix; the computational complexity reaches to $O(n^2m)$, where $O(\circ)$ is Landau's symbol, which means the rate of floating-point operations' growth. Besides, after k eigenvalues are obtained by IRAM, the left eigenvector associated with each distinctive eigenvalue has to be calculated by solving the linear problem as described in [26]. Additional LU factorization is inevitable with computational complexity of $O(n^3)$. Finally, sensitivity calculation would cost $k(n+1)$ times of n-dimension vector multiplication and a Bubble sort method also needs to be executed to realize finding of the most sensitive eigenvalues, of which the average computational complexity is $O(n^2)$. For example, the total CPU time for finding the most sensitive eigenvalues of system operating parameter's perturbation for a single shift point using IRAM with Krylov subspace dimension 100, $k = 50$ and $l = 4$ is 1446.17s. The CPU time for the generalized TSA-SPA is 248.97s as shown in Table XIII.

It is worth noting that the generalized TSA-SPA aims at

calculating sensitive eigenvalues in the vicinity of the shift point so the result is a compromise between the sensitivity of the calculated eigenvalues and the closeness of the calculated eigenvalues and the shift point. As shown in Table IX and Table XI, the four most sensitive eigenvalues calculated may not be the same as the four most sensitive eigenvalues listed in Table VIII and Table X.

TABLE VI
SENSITIVE INTER-AREA MODES OBTAINED BY GENERALIZED TSA-SPA BY SHIFT POINT (-0.1258, 2.5133) UNDER CONTROL PARAMETER PERTURBATION

Deflation number	Eigenvalue	Sensitivity (10^{-2})	State variable with max PF
0	-0.1134 + j2.6185	-0.1344 – j0.0417	ω_{87456}
1	-0.2225 + j1.6383	-0.0231 + j0.0052	ω_{87456}
2	-0.1261 + j2.8236	-0.0180 + j0.0061	ω_{87456}
3	-0.1231 + j2.3018	0.0487 – j0.0039	ω_{87456}

TABLE VII
SENSITIVE LOCAL MODES OBTAINED BY GENERALIZED TSA-SPA BY SHIFT POINT (-0.5347, 10.6814) UNDER CONTROL PARAMETER PERTURBATION

Deflation number	Eigenvalue	Sensitivity (10^{-2})	State variable with max PF
0	-0.9130 + j10.8538	-6.5794 – j0.0329	ω_{87456}
1	-0.1651 + j11.4636	-1.8720 – j0.0211	ω_{87456}
2	-0.6325 + j10.5189	-0.0126 – j0.0031	ω_{62032}

TABLE VIII
SENSITIVE EIGENVALUES (ELECTROMECHANICAL MODES) OBTAINED BY IRAM UNDER OPERATING PARAMETER PERTURBATION

Ranking number	Eigenvalue	Sensitivity (10^{-4})
1	-0.1646 + j3.7277	9.3437 – j1.1188
2	-0.0665 + j3.6905	2.1699 – j0.9641
3	-0.1260 + j2.8258	0.6696 – j2.2007
4	-0.5767 + j2.0371	0.8897 – j0.8206
5	-0.0888 + j3.0493	0.1019 + j1.1185
6	-0.1706 + j1.9204	-0.7631 + j0.0562
7	-0.7447 + j1.3225	-0.5359 – j0.5097
8	-0.5737 + j2.3039	0.0837 + j1.0593
9	-0.1123 + j2.6182	-0.1809 + j0.5620
10	-0.2224 + j1.6380	-0.1566 + j0.5546

TABLE IX
SENSITIVE INTER-AREA MODES OBTAINED BY GENERALIZED TSA-SPA WITH SHIFT POINT (-0.0943, 3.1416) UNDER OPERATING PARAMETER PERTURBATION

Deflation number	Eigenvalue (symbol)	Sensitivity (10^{-4})	State variable with max PF
0	-0.0888 + j3.0493 (Star ∗)	0.1145 + j1.1173	δ_{63590}
1	-0.0665 + j3.6905 (Square ■)	2.1708 – j0.9461	δ_{63590}
2	-0.1646 + j3.7277 (Dot ●)	9.3455 – j1.1021	ω_{63590}
3	-0.1260 + j 2.8258 (Circle ○)	0.6584 – j2.2083	δ_{87456}

TABLE X
SENSITIVE EIGENVALUES (ELECTROMECHANICAL MODES) OBTAINED BY IRAM UNDER NETWORK PARAMETER PERTURBATION

Ranking number	Eigenvalue	Sensitivity (10^{-1})
1	-0.0665 + j3.6905	0.9813 – j2.6354
2	-0.1254 + j2.2982	1.4276 + j1.8352
3	-0.1006 + j3.4653	0.2617 + j1.5435
4	-0.1103 + j2.6059	0.9565 + j0.6314
5	-0.1646 + j3.7277	0.3519 – j0.2516
6	-0.2224 + j1.6382	-0.0035 + j0.2496
7	-1.4315 + j2.0070	0.0431 – j0.2297
8	-0.7447 + j1.3225	-0.2143 + j0.0275
9	-0.1260 + j2.8258	0.0473 + j0.1767
10	-0.1123 + j2.6182	0.0307 + j0.1115

TABLE XI
SENSITIVE INTER-AREA MODES OBTAINED BY GENERALIZED TSA-SPA WITH SHIFT POINT (-0.0943, 3.1416) UNDER NETWORK PARAMETER PERTURBATION

Deflation number	Eigenvalue	Sensitivity (10^{-1})	State variable with max PF
0	-0.1006 + j3.4653	0.2642 + j1.5473	δ_{72869}
1	-0.0665 + j3.6905	0.9822 – j2.6350	δ_{63590}
2	-0.1646 + j3.7277	0.3520 – j0.2537	δ_{63590}
3	-0.1103 + j2.6059	0.9553 + j0.6335	δ_{87456}

TABLE XII
RELATIVE ERROR (RE) OF EIGENVALUE AND SENSITIVITY OBTAINED BY GENERALIZED TSA-SPA COMPARED WITH THAT OBTAINED BY IRAM

Table No.	Deflection No.	Eigenvalue	RE of eigenvalue (10^{-5})	RE of sensitivity (10^{-2})
VI	0	-0.1134 + j2.6185	0.4578	0.2008
	1	-0.2225 + j1.6383	4.5968	1.3204
	2	-0.1261 + j2.8236	2.1228	3.3265
	3	-0.1231 + j2.3018	2.0245	1.2965
VII	0	-0.9130 + j10.8538	0.6488	0.0096
	1	-0.1651 + j11.4636	0.8257	0.0107
	2	-0.6325 + j10.5189	1.1261	2.8531
IX	0	-0.0888 + j3.0493	4.6767	1.1269
	1	-0.0665 + j3.6905	4.5154	0.7590
	2	-0.1646 + j3.7277	5.1099	0.1785
	3	-0.1260 + j 2.8258	5.5891	0.5884
XI	0	-0.1006 + j3.4653	2.8844	0.2905
	1	-0.0665 + j3.6905	4.1162	0.0350
	2	-0.1646 + j3.7277	3.6827	0.4860
	3	-0.1103 + j2.6059	1.1911	0.2110

TABLE XIII
COMPUTATION COST OF GENERALIZED TSA-SPA UNDER SYSTEM OPERATING PARAMETER AND NETWORK PARAMETER PERTURBATION

Perturbation	Krylov subspace dimension	k	l	Iteration	CPU time (s)
Control Parameter	100	50	4	175+175+(5+8+15+21)	264.55
	100	50	5	175+175+(5+8+15+21+34)	264.58
	100	50	6	175+175+(5+8+15+21+34+45)	264.61
	200	50	4	207+207+(5+9+10+15)	371.94
	200	50	5	207+207+(5+9+10+15+26)	371.95
	200	50	6	207+207+(5+9+10+15+26+37)	371.97
System Operating Parameter	100	50	4	150+150+(6+6+10+18)	248.97
	100	50	5	150+150+(6+6+10+18+26)	248.99
	100	50	6	150+150+(6+6+10+18+26+42)	249.02
	200	50	4	200+200+(6+11+18+27)	397.41
	200	50	5	200+200+(6+11+18+27+40)	397.42
	200	50	6	200+200+(6+11+18+27+40+43)	397.43

	100	50	4	150+150+(6+9+20+39)	265.56
	100	50	5	150+150+(6+9+20+39+40)	265.58
	100	50	6	150+150+(6+9+20+39+40+42)	265.61
Network Parameter	200	50	4	200+200+(6+10+28+45)	373.93
	200	50	5	200+200+(6+10+28+45+40)	373.94
	200	50	6	200+200+(6+10+28+45+40+42)	373.95

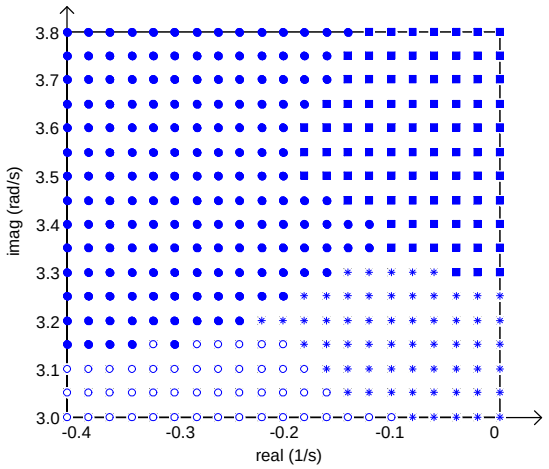

Fig. 3. Sensitive inter-area modes obtained by generalized TSA-SPA for different shift points

VI. Conclusion

This paper successfully generalizes the TSA-SPA to compute sensitive eigenvalues with respect to different types of parameter changes. Without forming the state matrix under perturbation, the proposed algorithm has advantage over TSA-SPA, being capable of coping with the perturbation at algebraic equations in large-scale power system's dynamic models and it does not limit the application by control parameters like the TSA-SPA. Pre-condition transformation is also applicable to the proposed method to focus on sensitive eigenvalues in a specified region of interest in complex plane. Other sensitive eigenvalues in the region can also be calculated with the proposed deflation technique. Numerical simulations confirm that the proposed algorithm is efficient and robust in computing sensitive eigenvalues in large-scale power systems. The proposed algorithm can provide a practical and effective analytical tool for power engineers to study the relationship between the stability problem and different parameters in large-scale power systems.

References

[1] H. D. Chiang, I. Dobson, R. J. Thomas, J. S. Thorp, and L. Fekihahmed, "On voltage collapse in electric-power systems," *IEEE Trans. Power Syst.*, vol. 5, pp. 601-611, May 1990.

[2] R. A. Jabr, B. C. Pal, and N. Martins, "A sequential conic programming approach for the coordinated and robust design of power system stabilizers," *IEEE Trans. Power Syst.*, vol. 25, pp. 1627-1637, Aug 2010.

[3] I. Kamwa, G. Trudel, and L. Gerin-Lajoie, "Robust design and coordination of multiple damping controllers using nonlinear constrained optimization," *IEEE Trans. Power Syst.*, vol. 15, pp. 1084-1092, Aug 2000.

[4] M. Zarghami, M. L. Crow, and S. Jagannathan, "Nonlinear control of FACTS controllers for damping interarea oscillations in power systems," *IEEE Trans. Power Delivery*, vol. 25, pp. 3113-3121, Oct 2010.

[5] C. Luo and V. Ajjarapu, "Sensitivity-based efficient identification of oscillatory stability margin and damping margin using continuation of invariant subspaces," *IEEE Trans. Power Syst.*, vol. 26, pp. 1484-1492, Aug 2011.

[6] D. P. Ke and C. Y. Chung, "An inter-area mode oriented pole-shifting method with coordination of control efforts for robust tuning of power oscillation damping controllers," *IEEE Trans. Power Syst.*, vol. 27, pp. 1422-1432, Aug 2012.

[7] D. P. Ke, C. Y. Chung, and Y. S. Xue, "An eigenstructure-based performance index and its application to control design for damping inter-area oscillations in power systems," *IEEE Trans. Power Syst.*, vol. 26, pp. 2371-2380, Nov 2011.

[8] H. Z. Huang, C. Y. Chung, K. W. Chan, and H. Y. Chen, "Quasi-monte carlo based probabilistic small signal stability analysis for power systems with plug-in electric vehicle and wind power integration," *IEEE Trans. Power Syst.*, vol. 28, pp. 3335-3343, Aug 2013.

[9] J. B. Zhang, C. Y. Chung, and Y. D. Han, "A novel modal decomposition control and its application to PSS design for damping interarea oscillations in power systems," *IEEE Trans. Power Syst.*, vol. 27, pp. 2015-2025, Nov 2012.

[10] J. B. Zhang, C. Y. Chung, S. Q. Zhang, and Y. D. Han, "Practical wide area damping controller design based on ambient signal analysis," *IEEE Trans. Power Syst.*, vol. 28, pp. 1687-1696, May 2013.

[11] H. Khalilinia, and V. Venkatasubramanian, "Modal analysis of ambient PMU measurements using orthogonal wavelet bases," *IEEE Trans. Smart Grid*, vol. 99, 2015, In Early Access.

[12] S. Dasgupta, M. Paramasivam, U. Vaidya, and V. Ajjarapu, "PMU-Based Model-Free Approach for Real-Time Rotor Angle Monitoring," *IEEE Trans. Power Syst.*, vol. 99, 2015, In Early Access.

[13] J. Ma, Z. Y. Dong, and P. Zhang, "Comparison of BR and QR eigenvalue algorithms system small signal stability analysis," *IEEE Trans. Power Syst.*, vol. 21, pp. 1848-1855, Nov 2006.

[14] R. T. Byerly, R. J. Bennon, and D. E. Sherman, "Eigenvalue analysis of synchronizing power flow oscillations in large electric-power systems," *IEEE Trans. Power App. Syst.*, vol. 101, pp. 235-243, 1982.

[15] D. Y. Wong, G. J. Rogers, B. Porretta, and P. Kundur, "Eigenvalue analysis of very large power systems," *IEEE Trans. Power Syst.*, vol. 3, pp. 472-480, May 1988.

[16] N. Uchida and T. Nagao, "A new eigen-analysis method of steady-state stability studies for large power systems: S Matrix Method," *IEEE Trans. Power Syst.*, vol. 3, pp. 706-714, May 1988.

[17] A. Semlyen and L. Wang, "Sequential computation of the complete eigensystem for the study zone in small signal stability analysis of large power systems," *IEEE Trans. Power Syst.*, vol. 3, pp. 715-725, May 1988.

[18] N. Martins, L. T. G. Lima, and H. J. C. P. Pinto, "Computing dominant poles of power system transfer functions," *IEEE Trans. Power Syst.*, vol. 11, pp. 162-167, Feb 1996.

[19] J. Rommes and N. Martins, "Computing large-scale system eigenvalues most sensitive to parameter changes, with applications to power system small-signal stability," *IEEE Trans. Power Syst.*, vol. 23, pp. 434-442, May 2008.

[20] Y. Saad, *Numerical Methods for Large Eigenvalue Problems, Revised Edition*. Manchester: Manchester University Press, 2011.

[21] C. Y. Chung and B. Dai, "A combined TSA-SPA algorithm for computing most sensitive eigenvalues in large-scale power systems," *IEEE Trans. Power Syst.*, vol. 28, pp. 149-157, Feb 2013.

[22] P. Kunder, *Power System Stability and Control*: McGraw-Hill, USA, 1994.

[23] K. Meerbergen and D. Roose, "Matrix transformations for computing rightmost eigenvalues of large sparse non-symmetric eigenvalue problems," *SIMA. J. Numer. Anal.*, vol. 16, pp. 297-346, Jul 1996.

[24] J. Cullum and T. Zhang, "Two-sided Arnoldi and nonsymmetric Lanczos algorithms," *SIAM J. Matrix Anal. Appl.*, vol. 24, pp. 303-319, Dec 19 2002.

[25] J. H. Wilkinson, *The Algebraic Eigenvalue Problem*: Clarendon Press, 1965.

[26] J. Rommes and N. Martins, "Efficient computation of transfer function dominant poles using subspace acceleration," *IEEE Trans. Power Syst.*, vol. 21, pp. 1218-1226, Aug 2006.

[27] J. Rommes and N. Martins, "Efficient computation of multivariable transfer function dominant poles using subspace acceleration," *IEEE Trans. Power Syst.*, vol. 21, pp. 1471-1483, Nov 2006.

[28] L. Wang, F. Howell, P. Kundur, C. Y. Chung, and X. Wilsun, "A tool for small-signal security assessment of power systems," in *Power Industry Computer Applications, 2001. PICA 2001. Innovative Computing for Power - Electric Energy Meets the Market. 22nd IEEE Power Engineering Society International Conference on*, 2001, pp. 246-252.

C. Y. Chung (M'01–SM'07) received the B.Eng. degree (with First Class Honors) and the Ph.D. degree in electrical engineering from The Hong Kong Polytechnic University, Hong Kong, China, in 1995 and 1999, respectively.

He worked in Powertech Labs, Inc., Surrey, BC, Canada, the University of Alberta, Edmonton, AB, Canada, and The Hong Kong Polytechnic University, China. He is currently a Professor and the SaskPower Chair in Power Systems Engineering in the Department of Electrical and Computer Engineering at the University of Saskatchewan, Saskatoon, SK, Canada. His research interests include power system stability/control, planning and operation, computational intelligence applications, power markets, and electric vehicle charging.

Dr. Chung is an Editor of the IEEE TRANSACTIONS ON SUSTAINABLE ENERGY and an Editorial Board Member of IET GENERATION, TRANSMISSION & DISTRIBUTION. He is also a Member-at-Large (Smart Grid) of IEEE PES Governing Board and the IEEE PES Region 10 North Chapter Representative.

Bo Dai (M'12) received the PhD degrees in electrical engineering from North China Electric Power University, Beijing, China, in 2009. Currently, she is working as a postdoctoral fellow in Department of Electrical Engineering, The Hong Kong Polytechnic University, Hong Kong, China.